**ACCEPTED VERSION**

Donnelley, Martin William; Siu, Karen K. W.; Jamison, R. A.; Parsons, David Webb
Synchrotron phase-contrast X-ray imaging reveals fluid dosing dynamics for gene transfer into mouse airways, Gene Therapy, 2012; 19(1):8-14.

© 2012 Macmillan Publishers Limited. All rights reserved.

**PERMISSIONS**

http://www.nature.com/gt/for_authors.html#Journal-open

- Authors of original research articles are encouraged to submit the author's version of the accepted paper (the unedited manuscript) to their funding body's archive, for public release six months after publication. In addition, authors are encouraged to archive this version of the manuscript in their institution's repositories and on their personal websites, also six months after the original publication. This is in line with NPG's self-archiving policy..

31st January 2014

**http://hdl.handle.net/2440/70264**

# Synchrotron phase contrast X-ray imaging reveals fluid dosing dynamics for gene transfer into mouse airways

**Martin Donnelley[1,5,6], Karen KW Siu[2,3], R Aidan Jamison[4] and David W Parsons[1,5,6,7]**

*[1]Respiratory and Sleep Medicine, Child, Youth and Women's Health Service, Adelaide, Australia*

*[2]Monash Centre for Synchrotron Science, Monash University, Victoria, Australia*

*[3]School of Physics, Monash University, Victoria, Australia*

*[4]Division of Biological Engineering, Monash University, Victoria, Australia*

*[5]Centre for Stem Cell Research, University of Adelaide, Australia*

*[6]Department of Paediatrics and Reproductive Health, University of Adelaide, Australia*

*[7]Women's and Children's Health Research Institute, Adelaide, Australia*

**CORRESPONDING AUTHOR CONTACT INFORMATION:**

Address: 72 King William Road, North Adelaide, SA 5006, Australia
Phone: +618 8161 7241
Fax: +618 8161 7050
Email: martin.donnelley@adelaide.edu.au

**RUNNING HEAD:**

Visualising fluid dosing dynamics in mouse airways

5590 Words

**ABSTRACT**

Although airway gene transfer research in mouse models relies on bolus fluid dosing into the nose or trachea the dynamics and immediate fate of delivered gene transfer agents are poorly understood. In particular this is because there are no *in vivo* methods able to accurately visualize the movement of fluid in small airways of intact animals. Using synchrotron phase-contrast X-ray imaging we show that the fate of surrogate fluid doses delivered into live mouse airways can now be accurately and non-invasively monitored with high spatial and temporal resolution. This new imaging approach can help explain the non-homogenous distributions of gene expression observed in nasal airway gene transfer studies, suggests that substantial dose losses may occur at delivery into mouse trachea via immediate retrograde fluid motion, and shows the influence of the speed of bolus delivery on the relative targeting of conducting and deeper lung airways.

These findings provide insight into some of the factors that can influence gene expression *in vivo*, and this method provides a new approach to documenting and analyzing dose delivery in small animal models.

**KEYWORDS**

X-ray imaging; high resolution; mouse; airways; instillation; gene transfer

## INTRODUCTION

The mouse respiratory system is widely used for the modeling of disease and treatment using live pathogens (bacterial, viral and fungal), pollutant particles, pharmaceuticals, allergens and gene therapies. Our group uses the mouse nose and lung as *in vivo* model sites for developing a gene therapy treatment for cystic fibrosis (CF) airway disease.[1,2] Reporter genes and/or the therapeutic (CFTR) gene contained in a lentiviral gene vector are delivered by *in vivo* bolus instillation into the nose and trachea. To produce lasting gene expression after a single dose event we utilize a 4 µl 0.1 – 1% (typically 0.3%) lysophosphatidylcholine (LPC) airway pre-treatment before delivering a 20 µl lentiviral gene vector dose (typically $10^7$ – $10^9$ tu/ml) to the mouse nose.[1-4] Reliable dosing is essential for the success of these airway gene transfer protocols, but despite the use of standardized delivery techniques our group and others report large variability in reporter gene histological assessments and in electrophysiological gene transfer measurements.[2,5,6] One cause of this variability may be the heterogeneous dose distribution that may occur in the physically complex nose and trachea.

The ability of standard imaging modalities to visualize the fluid dynamics in the mouse nose and lung is limited by their spatial and temporal resolution and their poor ability to discriminate soft tissues from air-containing structures in 2-dimensional imaging modes. Small-animal CT, and to a lesser extent MRI, which provide 3-dimensional (3D) information via tomographic approaches, could be used to examine murine airways but the time to acquire 3D data sets prohibits tracking of high speed dynamic events such as fluid dosing at high spatial resolutions. Although PET-CT has been used to show the final location of trans-nasally delivered solutions[7], the acquisition speed and spatial resolution of PET is very low, the dynamics of the fluid delivery cannot be imaged, the air containing spaces are poorly defined by CT and the spatial resolution is insufficient. None of these methods can visualize fluid movement in mouse airways at high resolution.

Synchrotron phase contrast X-ray imaging (PCXI)[8,9] is able to monitor the fate of a fluid dose bolus – similar to those used in our gene transfer studies – in the time immediately after delivery

with high temporal and spatial resolution. Synchrotron X-rays are electromagnetic radiation generated by the acceleration of ultra-relativistic (i.e. close to the speed of light) electrons through magnetic fields. PCXI provides enhanced image contrast by utilizing X-ray refraction in addition to conventional X-ray absorption and is particularly useful for achieving soft tissue contrast even where the absorption differences are small. The technique requires a spatially coherent source of X-rays, which is readily achievable using a synchrotron due to its intrinsically small source size. Tissue/air boundaries in particular are enhanced by the phase changes induced by their differences in X-ray refractive indices.[8,9] We have previously demonstrated the advantages of PCXI for small animal airway surface imaging[10,11] and for monitoring the post-deposition behavior of particulates on live mouse nasal and tracheal airways.[12,13] In this study we used PCXI to precisely and non-invasively track how introduced fluids, typical of those used in airway dosing, move through the airways of live and intact small animals.

We hypothesized that the effectiveness of the initial targeting and the distribution of a dose in live mouse airways could be determined for the first time by recording the immediate fate of instilled fluids in the nose and trachea. This study shows that the spread of the dose, the effectiveness of the delivery method and the persistence of the delivered dose could be visualized. Furthermore, the effects of altered dose volume and speed of delivery were also visible. This method now enables the rational design of more effective delivery procedures in the airway gene transfer protocols used in normal and CF mouse models.[1,2,14,15] It should also permit improvements in reliability and repeatability to boost outcome effectiveness, reduce outcome variability, and decrease the volumes of costly gene vectors needed in mouse model studies.

## RESULTS

No methods have been available to show the detailed fate of gene therapy fluid doses in the period immediately after delivery into mouse nose or trachea. The primary advance here was the coupling of an iso-osmotic iodine-based contrast fluid, mimicking our gene transfer dosing protocol, with synchrotron PCXI. Together they enabled direct and non-invasive visualization of the dynamics of the fluid delivery at a resolution that permitted reliable identification of the specific airway anatomy and regions affected. PCXI also provided unambiguous visualization of the complexity of the targeted nasal airways and trachea,[10] while also enhancing the boundary between the air and instilled contrast medium. We utilized a remote delivery apparatus to provide reliable initiation and duration of dosing and found that the 1:1 mixture of water and contrast fluid was well-tolerated by the anaesthetized mice. Only occasional respiratory perturbations occurred with the large volume deliveries, at a similar incidence to that experienced during our gene transfer studies.

During the experiments the incident photon flux was approximately $1.5 \times 10^8$ photons/sec/mm$^2$, producing a radiation dose of approximately 2 mGy for each 100 ms exposure. To the mouse this dose is comparable to a single human skull X-ray.[16]

### Nasal dose delivery

Figure 1 shows the position of the instilled 4 µl dose (a surrogate for our LPC pre-treatment) in six different mice 10 seconds after the completion of the standard 10 second fluid delivery. The pseudo-coloring shows where contrast fluid is present in the nasal airway and is created from the difference in contrast between the current and pre-delivery image frames. Fluid was taken up into the airway via normal tidal breathing, as occurs in our gene transfer dosing protocols. It is apparent that mice N1 to N4 show a very similar fluid distribution pattern in the lateral and posterior regions of the right nasal cavity. Compared to the anterior nostril region, far less fluid reaches the edge of the centrally-placed septum than moves laterally. Note that in mouse N3 fluid is also present along the lateral edge of the right airway and the amount of lateral right-nostril fluid is reduced. Supplementary Video 1 shows the spread of fluid within the nasal airways of all six mice as the

dose is progressively expelled from the nearby cannula. Two mice (N5 and N6 in Figure 1) show the effect of incomplete nasal dose deliveries, caused by an adherent fluid droplet forming at the cannula tip. In mouse N6 the droplet bridges across to the nostril and is suddenly inhaled, immediately extending the distribution of fluid into the right nasal cavity. In mouse N5, the droplet remains at the tip throughout (see also Figure 2 below, where the fluid droplet is still present 10 minutes later); this lower delivered volume prevented fluid reaching the more posterior regions of the right nasal airway when compared to mice N1, N2 and N4. In mouse N3 some fluid travelled along the right side of the nasopharyngeal meatus (NPM) causing a reduction in the dose retained within the right nasal anterior airway. Despite the variability fluid was still present in the nasal cavities of all mice 10 minutes after the initial 4 µl delivery.

Figure 2 shows the effects of a subsequent 20 µl dose (a surrogate for our lentiviral vector) delivered into the same mice (N1-N5). Images were processed such that the contrast fluid remaining 10 minutes after the 4 µl delivery was considered to be background, enabling the dynamics of this second dose bolus to be easily seen. These images show a wider dose distribution extending into the nasopharynx and past the epiglottis, as might be expected from addition of a larger dose. The dynamics of this second dose delivery are shown in Supplementary Video 2. We were surprised to observe the extensive and rapid filling of the NPM, the cyclical nature of bulk fluid movement up and down the nasal airway, the creation of both small and full-width gas bubbles, and the ability of this 20 µl dose to pass the epiglottis and enter the trachea. In addition, some fluid also reaches into the pharynx and the oral cavity where it is evident as large bubble edges that are wider than the boundaries of the posterior nasopharyngeal airway. This is best observed in some of the later image frames for mouse N2. Cessations of nasal airway fluid movement in these spontaneously respiring mice were also noted after the 20 µl dose, visible as almost stationary airway bubbles, air gaps, or fluid within the nasopharynx across a number of frames in mice N1 (25 to 53 seconds), N2 (14 to 32 seconds) and N3 (16 to 57 seconds) in Supplementary Video 2.

**Lung dose delivery**

The captured image frames required different processing to the nasal airway images. We displayed the fluid position (in yellow-blue pseudo-color) by calculating the intensity change *between* frames, thereby minimizing the effects of any general body and lung movement throughout the experiment (see Supplementary Video 3). Figure 3 shows where instilled fluid was present two breaths (2.25 seconds) after the initiation of a 30 second delivery of 15 µl of fluid via the dosing cannula. For clarity the tips of the ET tube and the smaller diameter dosing cannula are both marked in one mouse (L1). Of particular note is the immediate retrograde movement of the fluid from the cannula tip in each animal (see breaths zero to eight in Supplementary Video 3), although the manner of movement was different. For example, in mouse L1 the dose tracked back along the cannula outer wall, in mice L2 and L4 fluid also spread onto one side the tracheal wall, and in mouse L3 fluid spread to both tracheal walls. Figure 5 shows an example of the dynamics of lung fluid delivery (images were captured at 1.33 Hz from mouse L1 in Figure 3, and were extracted from Supplementary Video 3) as a portion of the fluid dose moves down the left main bronchus.

To determine how a faster delivery rate affected the distribution dynamics we delivered the same 15 µl volume over a 3.6 second period, the maximum flow rate of the infusion pump (Figure 4). This fast fluid bolus delivery (images in Figure 4 extracted from Supplementary Video 4) created larger localized increases in the contrast fluid volume that were more easily visualized. The video sequences show localized boluses progressing along both the left and right main bronchi. The ensuing spread of the contrast bolus onto bases of the respective lung lobes is shown by the rapid loss of contrast, probably due to splitting of the bolus into smaller airways in the base of this lobe. This faster dosing method clearly delivered more fluid more rapidly into the small airways of the lung lobes than the slower delivery.

Although entire lung perturbations or small body movements could interfere with image analysis of dose delivery, they also show a direct effect of instilling fluid into a mouse airway. The small movements in the alveolar speckle pattern (which is greatly enhanced by PCXI )[17] during normal

respiration, as well as movement of the heart muscle, are sufficient to often partially obscure the movement of the contrast agent in airways. In some animals, such as mouse L3, the body movements were large enough to create “ghost” outlines of bones and organs, since the pseudo-color processing highlights all differences between frames (e.g. mouse L3, breaths 18, 41 and 58 in Supplementary Video 3).

## DISCUSSION

The primary goal of this study was to document and understand the dynamics of fluid bolus dose delivery into the nose and trachea of live mice using synchrotron PCXI. This is the first method we are aware of able to provide high resolution non-invasive imaging of dosing dynamics in live intact mice. It has the potential to improve the effectiveness and reduce the variability of gene therapy protocols where despite standardized procedures inconsistent levels and distributions of cell transduction are experienced in mouse nose and lung.[1,2,4] This new ability to directly visualize the delivery of a fluid in the airway at high temporal and spatial detail also suggests an immediate relevance and utility to other respiratory health and disease research modeling applications in small animals when pharmaceutical, infectious, allergenic and particulate fluid installations are utilized.

This PCXI data can now help explain some of the patterns of gene expression produced by our gene transduction protocols in living mouse airways. Only the nasal epithelium in transgenic cystic fibrosis mice is suited to CF airway gene transfer modeling;[18] in our studies we utilize a 4 µl LPC pre-treatment followed by a 20 µl lentiviral vector dose.[1-4] When correctly delivered (Figure 1, mice N1 and N2) the 4 µl volume remained on the treated side of the nasal cavity. In mouse N3 fluid can also be seen in the nasopharynx, but only along the treated side of the nasal airway. These results validate the use of a 4 µl dose (originally estimated by scaling down dose volumes established in rats[19] based on typical mouse body weights) to dose one anterior nasal airway while simultaneously retaining an untreated (left) nasal airway to act as an unexposed, within-animal control airway for nasal airway studies. Furthermore, the results suggest that in those rare cases where gene expression extended into the nasopharynx (see Limberis, et. al.,[4] and the cover photo of that issue), the expression was limited to the treated side, i.e. only to those areas where the 4 µl LPC pre-treatment had reached. The retention (rather than rapid loss) of a 4 µl dose within both the respiratory and olfactory epithelial regions of the treated nostril supports, firstly, the strength and reliability of gene expression we have observed in nasal ciliated epithelium. Secondly, it suggests that the absence of transduced (non-target) olfactory epithelium from our VSV-G pseudotyped lentiviral gene vector[2,4] occurs despite the vector dose distributing into and being retained in this

mixed transitional/olfactory region. This distribution is also consistent with the off-target transduction of olfactory tissue produced by other vectors (e.g. AdV, FIV, etc).[14,20] Finally, the lower levels of gene expression we observe on the nasal septum compared to the lateral ciliated regions are consistent with the differences in fluid retention in these two regions. The ability to observe where the dose is retained, or the tissue-type targeted,[21] should be useful in the testing of pharmaceuticals, infectious agents, allergens and other gene vectors in these different epithelial tissues. The visualization of partial dose delivery distributions also suggests that whenever incomplete or inconsistent dosing (e.g. nostril bridging or sneezing) is noted gene transduction is likely to be affected. One recommendation from these findings is that to reduce outcome variability those animals that show partial dosing and/or sneezing or snorting of the dose should not be included in normal assessments.

The 20 µl nasal dose (equal to our lentiviral gene vector delivery volume) appears to overwhelm the 'holding capacity' of the pre-treated anterior right nostril region; this second nasal airway fluid delivery moved immediately into the nasopharynx. Supplementary Video 2 reveals a reciprocating fluid motion in some mice, with some fluid continuing past the epiglottis into the trachea. Although the anatomy below the upper trachea could not be imaged in this nasal airway study it is likely that fluid reached further into the lung airways, a finding consistent with a recent low-resolution radiotracer study.[7] The results also supports our finding that long term gene expression was produced in the lung by a lentiviral vector containing the luciferase transgene that was delivered to the nose and was designed specifically to produce *nasal* airway gene transfer.[22] It follows that smaller gene vector doses might be able to produce the same levels of gene expression in the anterior nasal airways.

Comparison of the distributions of the 4 µl and 20 µl volumes also supports the proposed mechanism of action of LPC pre-treatments. If LPC makes the airway surface receptive to gene vector uptake[3] we expect that vector transduction will only occur where LPC has previously reached and affected an airway-surface region. The unilateral nasal airway gene expression produced when using these protocols[2,4] is consistent with this notion since we only observe

patterns of gene expression in areas reached by the 4 µl dose, despite demonstrating the wide reach of the 20 µl (surrogate vector) dose throughout the entire nasopharynx. The nasopharynx epithelium is entirely ciliated respiratory epithelium[21] and it follows that if the nasopharynx could be effectively pre-treated around its full circumference with LPC, then homogeneous gene transduction might be achieved there. This novel lung airway-like site could potentially be used for modeling the effects of gene vectors or drugs on ciliated airway function within a tubular lung-like conducting airway, an option identified by others in related studies of mouse nasal electrophysiological function.[23] It should be noted that once fluid reaches the nasopharynx in sufficient volume to fill the airway diameter it is possible for retrograde fluid movement into the contralateral anterior nasal airway due to normal breathing or "sneezing" reactions that produce fluid movement into otherwise un-dosed airway regions.

Although most CF airway gene therapy research in mice is based on effects in ciliated nasal airway tissue[18] most murine respiratory research is naturally focused on the trachea, conducting airways and parenchyma. The current study showed how the speed of delivery can alter the way a fluid dose spreads into the lung tree. Although mice were oriented vertically the fluid was observed moving into the left, the right, or into both mainstem bronchi despite a standard dose-delivery protocol via an accurately placed tracheal dosing cannula. Of some note is that the first movement of fluid after it was slowly expelled from the cannula was retrograde, away from rather than down into the lung. The instilled fluid moved out of the airway against gravity, along or around the cannula body and/or on the adjacent tracheal wall, therefore reducing the intended volume delivered to the targeted distal conducting airways and parenchyma. The studies here were not designed to quantify these losses, but it is clear that it is important to monitor and document dose losses during lung instillations, since such losses may help explain the patchy gene expression distribution and the high variability we and others observe in lung dosing studies.

This new imaging method is broadly applicable. It now permits evidence-based attention to the design of mouse lung dosing protocols to improve the delivery to specific regions of the lung, for example, by linking the effect of incomplete dosing to its reach into regional airways. It could also

reveal how a defined smaller dose might be effectively targeted to more restricted regions of anterior nasal airway. More generally, it has the ability to provide an accurate and direct correlation between the effect of the delivery of a treatment dose and its outcome. The variations in outcome that result from changes in cannula placement, dose volume, timing of delivery (initiation of, and during the respiratory cycle), orientation of the mouse, and the speed of delivery could also be assessed using this technique.

The lung is a challenging organ to image accurately and precisely. Accurate detection of fluid motion in airways requires the regions of interest to be motionless, but for lung imaging this must be traded against the need to leave the lung structural elements free to move with respiration. Muscle paralysis agents were not employed here, and although gating image acquisition to the respiratory cycle was usually effective, this alone did not accommodate the small variations imposed on the rates of expansion or contraction of the lung, especially when these were perturbed by the fluid dosing itself. A 20 µl fluid dose introduced into a lung of approximately 300 µl tidal volume (a ~ 6.7 % volume change) sufficiently perturbed the regularity of the ventilator-driven lung movement such that all the lung lobes (e.g. mouse L1 in Supplementary Video 4) were strongly pseudo-colored, complicating data analysis and interpretation.

The large field of view and high resolution of the SPring-8 BL20B2 beamline affords a unique view of how a dosing fluid moves in a live intact respiratory system. In these experiments we chose to image at a low frame rate (1 Hz for the free breathing nasal studies, and at 1.33 Hz for lung as triggered by the ventilator) but in a separate study (data not shown) we have already imaged mouse lungs at nearly 30 Hz, sufficient to capture all stages of the respiratory cycle. Clearly, this new approach greatly improves on the capabilities of currently available imaging modalities in live animals both in terms of its spatial and temporal resolution, and in the ability to better visualize the air-containing anatomical structures. These capabilities provide considerably more imaging possibilities than systems utilizing a radiotracer,[7] which are substantially limited by the capture period (i.e. 40 seconds per frame) and spatial resolution (i.e. 0.81 mm isotropic voxels, 50 times larger than the pixel size used here). Since the radiation dose for a single image acquired during

this experiment was less than 2% of the total dose delivered in a single small animal micro-CT scan[24,25] this technique has the potential to be applied to studies designed to correlate how alterations in fluid dose delivery parameters can affect subsequent gene expression.

There are limitations that, when addressed in future studies, should further expand the potential of this technique. Mice were only oriented vertically (i.e. head high) here to match our current mouse airway gene transfer protocols,[2,4] providing a standard orientation and direct (or stereomicroscope) vision of cannula-based delivery to the nostril. However, there are a range of animal orientations used by other research groups,[26] and since orientation is a likely contributor to the diversity of outcomes of nasal airway gene transfer this technique can now provide precise comparisons of the effect of body orientation on dose-fluid distributions. The use of paralytic agents should also be considered to better limit confounding lung and body movements. Our method can also be used to ask similar questions in pollutant, allergen and infectious-agent studies in mouse lung. It may also assist in defining dose-delivery protocols better able to direct a dose to specific regions or lobes of the lung without introducing the confounding effects that potentially arise from deep cannula placement into airways, such as we have observed in gene transfer studies (see Liu et al[1] Figure 1e and 1f).

Although we diluted the contrast fluid to make it iso-osmotic with physiological saline, the delivered fluid had a slightly higher viscosity than isotonic sodium chloride.[27,28] In addition, the complex non-Newtonian properties and behavior of a two-phase viral gene vector may not be accurately mimicked by a single phase contrast agent. However, since each gene vector can have a different viscosity due to the influence of the diluent, the level of included proteins, and the concentration of vector particles, the viscosity is a characteristic that should be examined when considering the progression and intended destination of a dose moving through small airways where capillary forces issues may be significant. Since the viscosity affects the vector residence time,[29,30] and therefore the level of gene transduction, the effect of this key characteristic may now be quantified using this technique.

In summary, this non-invasive high resolution synchrotron PCXI technique for visualizing and analyzing fluid dose movement has for the first time provided gene therapy researchers the ability to ask and answer specific questions about the airway distribution dynamics of fluid doses delivered into live mouse nose and trachea. In a number of small animal models it could allow creation of standardized dosing protocols able to maximize and compare outcomes across different research groups while using the most appropriate volume of expensive gene vectors or other pharmaceutical agents.

## METHODS

Experiments were performed on the BL20B2 bending magnet beamline at the SPring-8 synchrotron radiation facility in Japan, under approvals from the Animal Ethics Committee of SPring-8, and of the Child, Youth and Women's Health Service, Adelaide. Mice were anaesthetized with pentobarbital (Somnopentil, Pitman-Moore, Washington Crossing, USA, 100 mg/kg i.p.) and then anesthesia was maintained by constant infusion of Nembutal (0.1 mg/kg/sec, via an indwelling i.p. needle) from a syringe pump (UltraMicroPump III and Micro4 controller, World Precision Instruments, Florida, USA). Body temperature was maintained using an infrared heat lamp and monitored with a rectal thermometer. Mice were anaesthetized for a total of less than one hour. After completion of each experiment mice were humanely killed via overdose of pentobarbital, without loss of anesthesia. Since mice remained anaesthetized prior to death no attempt was made to minimize radiation dose, rather we maximized both the number and quality of the images acquired.

### Imaging setup

The imaging hutch was located in the Biomedical Imaging Centre, 211 meters from the source,[31] and the imaging layout was as described previously,[10] Monochromatic 25 keV (λ=0.5Å) X-rays were selected using a Si(111) double-crystal monochromator to provide maximum flux at this energy,[32] A propagation (sample to detector) distance of ~2 m was chosen to produce optimal phase contrast for airway imaging. X-rays were converted to visible light using a P43 ($Gd_2O_2S$:Tb) scintillator and images were captured using a CCD detector (C9300-124F21, Hamamatsu Photonics) coupled to the scintillator using a fiber optic taper. The CCD detector had an array size of 4000 x 2672 pixels and a 9 x 9 µm native pixel size. This setup resulted in an effective isotropic pixel size of 16.2 µm. A sub-array of the CCD (1648 x 1936 pixels) was matched to the beam size at the sample position to give a field of view of approximately 27 mm x 31 mm. An exposure length of 100 ms was chosen to capture sufficient photons to fill the potential dynamic range ($2^{12}$ grey levels) of the detector, provide the maximal signal to noise ratio without detector saturation, and minimize blurring from animal movement.

**Nasal studies**

Six anaesthetized female C57/Bl6 mice (~20 grams) were individually secured head-high to a polyethylene imaging board[33] with the incisors hooked over a wire loop and the limbs, shoulders and lateral torso taped to the board to minimize body movements. The imaging area (head/torso) was brushed with a thin layer of glycerol to eliminate air in the fur layer (which would otherwise create a high signal in the images as PCXI is very sensitive to boundaries). The X-ray beam passed dorso-ventrally through the nose (and the lung, see below). A PE10 polyethylene cannula (SteriHealth, Melbourne, Australia) was positioned using a micromanipulator so its tip was 1-2mm above the right nostril, to simulate our normal (hand-delivered) nasal gene vector delivery setup.[1] A 1:1 mix of the iodine-based contrast agent iomeprol (Iomeron 350, Bracco-Eisai, Tokyo, Japan[28]) and water (to produce an osmolarity similar to 0.9% saline) was delivered through the cannula using a second UltraMicroPump III syringe pump, remotely activated from outside the imaging hutch. Priming of the syringe and PE tubing ensured accurate dose initiation and delivery. Fluid was taken into each mouse by its normal tidal volume inhalations and the cannula tip did not make contact with the mouse.

Images were captured at 1 Hz. After one minute of baseline collection, a 4 µl sample of the contrast mix (as a surrogate for our 4 µl gene transfer airway pre-treatment protocol)[2-4] was delivered in a single bolus over 10 seconds. Following 10 minutes of data collection an additional bolus of 20 µl (a surrogate for gene vector delivery) was delivered over 30 seconds. Image capture continued for a further 10 minutes, creating a 21 minute dataset consisting of a total of 1260 images per mouse covering 2 acute dose deliveries.

**Lung studies**

A similar protocol was used for the lung imaging. Four female C57/Bl6 mice (~20 grams) were anaesthetized then intubated with a 20Ga i.v. catheter (Insyte, Becton Dickinson, Utah, USA).[33] This endotracheal (ET) tube was inserted into the trachea to a nominal depth of 22.5mm from the nose tip, which placed the ET tube tip below the fifth cartilage ring (approximately half way between

the epiglottis and the carina). The Luer hub of the catheter was immediately cut off to enable the ET tube to be directly connected to the ventilator circuit and ensure respiratory dead-space was minimized. A flexiVent small animal ventilator (Scireq, Canada) provided ventilation set at 80 breaths/min with a tidal volume of 30 ml/kg (minute ventilation ~48 ml/min) and ~3 $cmH_2O$ of PEEP. The ventilatory profile was configured with $T_{inspiration}$ = 0.25 sec, $T_{pause}$ = 0.1 sec and $T_{expiration}$ = 0.4 sec to provide an end-inspiratory pause that matched the 100ms exposure length and minimized image motion artifacts. Doses were delivered via a heat-thinned PE10 polyethylene cannula placed inside the ET tube so that its tip extended 5mm below the end of the ET tube,[33] a similar depth to that used in our mouse lung gene transfer studies.[1] The same UltraMicroPump III syringe was used to remotely deliver the contrast mix via this smaller cannula.

Image capture was triggered by the ventilator at the beginning of every end-inspiratory pause, i.e. every 1.33 seconds. After 15 seconds of baseline collection (20 breaths), a 15 µl sample of the contrast mix (surrogate of LPC or vector) was delivered in a single bolus over 30 seconds. This dose volume has been used in our lung gene transfer studies[1]. After 20 minutes a second bolus of 15 µl was delivered over 3.6 seconds (the maximum rate of the syringe pump) to assess the effects of rapid delivery. Imaging continued for a further 4 minutes creating a 24 minute dataset consisting of a total of 1920 images per mouse.

**Post experimental analyses**

Each image sequence was flat-field and dark-field corrected and an image subtraction algorithm was used to locate changes in image brightness (Matlab 2009b, The Mathworks, USA). For the nasal studies the brightness difference was calculated by subtracting each frame from the baseline image five frames prior to delivery initiation (i.e. background subtraction of the mouse anatomy to reveal the fluid motion). A constant threshold of 128 grey values (1/32 the dynamic range) was then applied to select only the large intensity changes likely to correspond to fluid motion. The results were then 3x3 median-filtered to reduce noise prior to being used to pseudo-color the original images to show the presence and / or movement of the delivered fluid. The regions where the

image became darker (increasing presence of contrast fluid) were colored with a red to yellow color scale, and those that became lighter (decreasing presence of contrast fluid) were colored with a blue to purple color scale (see Figure 1). For the lung studies the brightness difference between successive frames (i.e. frame differencing) was calculated to compensate for the greater confounding movements produced by the constant respiratory and cardiac motion. Each frame was converted to an RGB image and the red, green and blue channels were adjusted to show the regions with more contrast fluid in yellow and the regions with less contrast fluid as light blue. This visualization method minimized the effects of body motion and eliminated the need to choose a different threshold for each animal that would complicate between-animal comparisons. For high quality motion-detection analysis the background must remain still compared to the foreground objects (here, the contrast fluid) to be detected, hence the special efforts we made to minimize the movement of the mouse during imaging, including the use of restraining boards and respiratory-gating as described above. Supplementary information is available at the Gene Therapy website.

## ACKNOWLEDGEMENTS

Studies supported by the NH&MRC Australia, with additional support from philanthropic donors via the CURE4CF Foundation (www.cure4cf.org). The synchrotron radiation experiments were performed on the BL20B2 beamline at SPring-8, with the approval of the Japan Synchrotron Radiation Institute (JASRI) under proposal number 2010A1523. Prof Naoto Yagi and Dr Kentaro Uesugi provided expert synchrotron imaging, X-ray and control advice and assistance at the SPring-8 synchrotron. We thank P. Cmielewski, M. Limberis and D. Miller for their editorial input. M.D., K.S., A.J. and D.P. supported by the International Synchrotron Access Program (ISAP) managed by the Australian Synchrotron. The ISAP is an initiative of the Australian Government being conducted as part of the National Collaborative Research Infrastructure Strategy.

## CONFLICT OF INTEREST

The authors declare no conflict of interest.

## AUTHOR CONTRIBUTIONS

D.P. conceived the research; M.D. and D.P. devised the experiments; M.D. and D.P. performed the animal experiments in conjunction with K.S. and A.J. who performed the synchrotron imaging; M.D. and D.P. conceived the image analyses; M.D. performed the image analyses and constructed the figures and supplementary material; M.D. and D.P. wrote the initial manuscript and all authors edited and approved the final version.

## REFERENCES


1. Liu C, Wong E, Miller D, Smith G, Anson D, Parsons D. Lentiviral airway gene transfer in lungs of mice and sheep: Successes and challenges. *The Journal of Gene Medicine* 2010; **12**(8)**:** 647-658.

2. Stocker A, Kremer K, Koldej R, Miller D, Anson D, Parsons D. Single-dose lentiviral gene transfer for lifetime airway gene expression. *The Journal of Gene Medicine* 2009; **11**(10)**:** 861-7.

3. Cmielewski P, Anson DS, Parsons DW. Lysophosphatidylcholine as an adjuvant for lentiviral vector mediated gene transfer to airway epithelium: Effect of acyl chain length. *Respiratory Research* 2010; **11:** 84.

4. Limberis M, Anson DS, Fuller M, Parsons DW. Recovery of airway cystic fibrosis transmembrane conductance regulator function in mice with cystic fibrosis after single-dose lentivirus-mediated gene transfer. *Human Gene Therapy* 2002; **13**(17)**:** 1961-1970.

5. Griesenbach U, Boyd AC. Pre-clinical and clinical endpoint assays for cystic fibrosis gene therapy. *Journal of Cystic Fibrosis* 2005; **4**(2)**:** 89-100.

6. Griesenbach U, Smith SN, Farley R, Singh C, Alton EW. Validation of nasal potential difference measurements in gut-corrected CF knockout mice. *Am J Resp Cell Mol* 2008; **39**(4)**:** 490-6.

7. Soto-Montenegro ML, Conejero L, Vaquero JJ, Baeza ML, Zubeldia JM, Desco M. Assessment of airway distribution of transnasal solutions in mice by PET/CT imaging. *Mol Imaging Biol* 2009; **11**(4)**:** 263-268.

8. Cloetens P, Barrett R, Baruchel J, Guigay JP, Schlenker M. Phase objects in synchrotron radiation hard X-ray imaging. *J Phys D Appl Phys* 1996; **29**(1)**:** 133-46.

9. Snigirev A, Snigireva I, Kohn V, Kuznetsov S, Schelokov I. On the possibilities of X-ray phase contrast microimaging by coherent high-energy synchrotron radiation. *Rev Sci Instrum* 1995; **66**(12)**:** 5486-5492.

10. Parsons DW, Morgan K, Donnelley M, Fouras A, Crosbie J, Williams I *et al.* High-resolution visualization of airspace structures in intact mice via synchrotron phase-contrast X-ray imaging (PCXI). *J Anat* 2008; **213**(2)**:** 217-227.

11. Siu KKW, Morgan KS, Paganin DM, Boucher R, Uesugi K, Yagi N *et al.* Phase contrast X-ray imaging for the non-invasive detection of airway surfaces and lumen characteristics in mouse models of airway disease. *Eur J Radiol* 2008; **68**(3)**:** S22-S26.

12. Donnelley M, Morgan K, Fouras A, Skinner W, Uesugi K, Yagi N *et al.* Real-time non-invasive detection of inhalable particulates delivered into live mouse airways. *Journal of Synchrotron Radiation* 2009; **16**(4)**:** 553-561.

13. Donnelley M, Morgan K, Skinner W, Suzuki Y, Takeuchi A, Uesugi K *et al.* A new technique to examine individual particle and fibre deposition and transit behaviour on live mouse trachea. *Journal of Synchrotron Radiation* 2010; **17:** 719-729.

14. Sinn PL, Arias AC, Brogden KA, McCray PB. Lentivirus cector can be readministered to nasal epithelia without blocking immune responses. *J Virol* 2008; **82**(21)**:** 10684-10692.

15. Mitomo K, Griesenbach U, Inoue M, Somerton L, Meng CX, Akiba E *et al.* Toward gene therapy for cystic fibrosis using a lentivirus pseudotyped with sendai virus envelopes. *Mol Ther* 2010; **18**(6)**:** 1173-1182.

16. Hart D, Hillier MC, Wall BF. National reference doses for common radiographic, fluoroscopic and dental X-ray examinations in the UK. *Br J Radiol* 2009; **82**(973)**:** 1-12.

17. Kitchen MJ, Paganin D, Lewis RA, Yagi N, Uesugi K, Mudie ST. On the origin of speckle in X-ray phase contrast images of lung tissue. *Phys Med Biol* 2004; **49**(18)**:** 4335-48.

18. Grubb BR, Boucher RC. Pathophysiology of gene-targeted mouse models for cystic fibrosis. *Physiol. Rev.* 1999; **79**(1 Suppl)**:** S193-214.

19. Chandler SG, Illum L, Thomas NW. Nasal absorption in the rat .1. A method to demonstrate the histological effects of nasal formulations. *Int J Pharmaceut* 1991; **70**(1-2)**:** 19-27.

20. Sinn PL, Burnight ER, Hickey MA, Blissard GW, McCray PB, Jr. Persistent gene expression in mouse nasal epithelia following feline immunodeficiency virus-based vector gene transfer. *J Virol* 2005; **79**(20)**:** 12818-27.

21. Mery S, Gross EA, Joyner DR, Godo M, Morgan KT. Nasal diagrams - a tool for recording the distribution of nasal lesions in rats and mice. *Toxicologic Pathology* 1994; **22**(4)**:** 353-372.

22. Cmielewski P, Anson DS, Parsons DW. Re-emergence of luciferase expression in lung following a single nasal instillation of a lentiviral vector in normal and cystic fibrosis mice. In: *J. Cyst. Fibros.* , 2010. p (S1) S17.

23. Grubb BR, Rogers TD, Boucher RC, Ostrowski LE. Ion transport across CF and normal murine olfactory and ciliated epithelium. *Am J Physiol-Cell Ph* 2009; **296**(6)**:** C1301-C1309.

24. Boone JM, Velazquez O, Cherry SR. Small-animal X-ray dose from micro-CT. *Mol Imaging* 2004; **3**(3)**:** 149-58.

25. Figueroa SD, Winkelmann CT, Miller WH, Volkert WA, Hoffman TJ. TLD assessment of mouse dosimetry during microCT imaging. *Med Phys* 2008; **35**(9)**:** 3866-3874.

26. Griesenbach U, Munkonge FM, Sumner-Jones S, Holder E, Smith SN, Boyd AC *et al.* Assessment of CFTR function after gene transfer in vitro and in vivo. *Methods Mol. Biol.* 2008; **433:** 229-42.

27. Gallotti A, Uggeri F, Favilla A, Cabrini M, de Haen C. The chemistry of iomeprol and physico-chemical properties of its aqueous solutions and pharmaceutical formulations. *Eur J Radiol* 1994; **18 Suppl 1:** S1-12.

28. Iomeron Data Sheet. From: Eisai Co., Ltd, Japan, 2009. http://www.eisai.jp/medical/products/di/EPI/IOM_V_EPI.pdf.

29. Griesenbach U, Meng C, Farley R, Wasowicz MY, Munkonge FM, Chan M *et al.* The use of carboxymethylcellulose gel to increase non-viral gene transfer in mouse airways. *Biomaterials* 2010; **31**(9)**:** 2665-72.

30. Sinn PL, Shah AJ, Donovan MD, McCray PB, Jr. Viscoelastic gel formulations enhance airway epithelial gene transfer with viral vectors. *Am J Resp Cell Mol* 2005; **32**(5)**:** 404-10.

31. Goto S, Takeshita K, Suzuki Y, Ohashi H, Asano Y, Kimura H *et al.* Construction and commissioning of a 215-m-long beamline at SPring-8. *Nucl Instrum Meth A* 2001; **467:** 682-685.

32. Yabashi M, Yamazaki H, Tamasaku K, Goto S, Takeshita K, Mochizuki T *et al.* SPring-8 standard X-ray monochromators. *Proc. SPIE* 1999; **3773:** 2-13.

33. Donnelley M, Parsons D, Morgan K, Siu K. Animals in synchrotrons: Overcoming challenges for high-resolution, live, small-animal imaging. *AIP Proceedings* 2010; **1266:** 30-34.

**FIGURES**

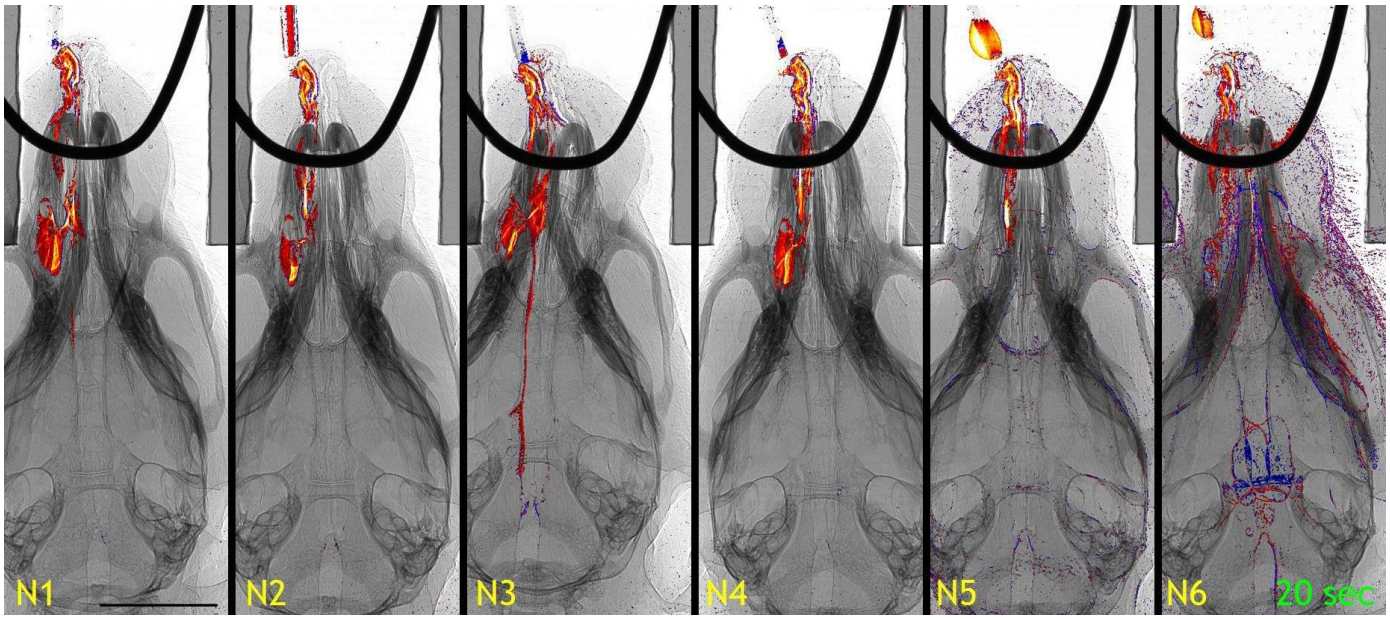


**Figure 1 | Four microliter fluid dose in mouse nasal airways**

Pseudo-colored images from the background subtraction algorithm showing the location of a 4 µl delivered dose of 1:1 iomeprol and water mix delivered over 10 seconds in six mice. Each image shows the fluid distribution 20 seconds after delivery initiation. Scale bar is 5 mm in all figures.

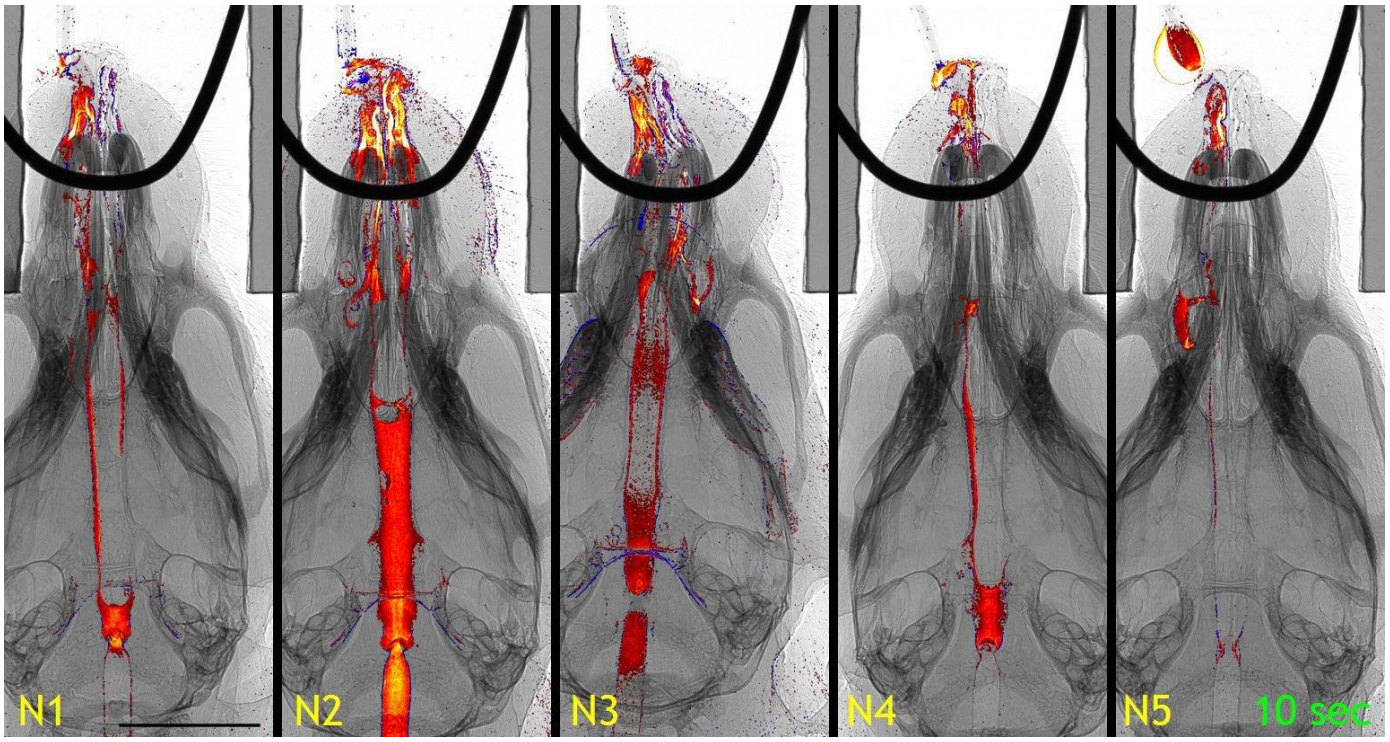


**Figure 2 | Twenty microliter fluid dose in mouse nasal airways**

Images from five mice (mouse N6 in Figure 1 died of unknown causes while under anesthesia just prior to this dose delivery) showing the location of a 20 µl dose that was delivered over 30 seconds. The images are taken at 10 seconds after delivery began.

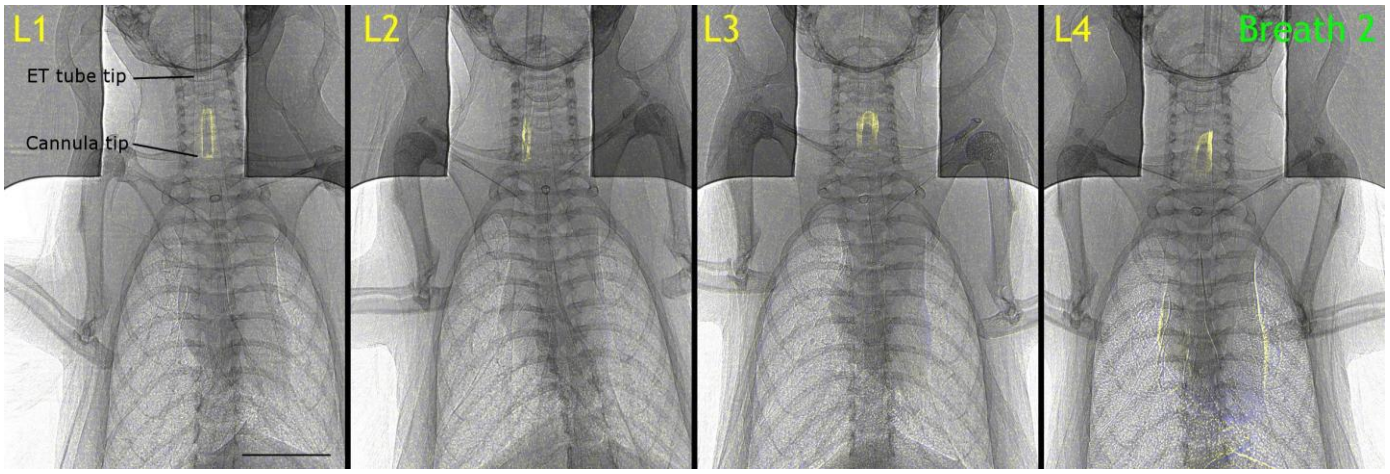


**Figure 3 | Fifteen microliter fluid dose in mouse trachea**

Images from the frame difference algorithm showing the location of the initiation of a 15 µl dose delivered slowly over 30 seconds (shown at two breaths after delivery initiation in 4 mice). The

location of the cannula tip and ET tube tip are marked for mouse L1. Images are taken from Supplementary Video 3.

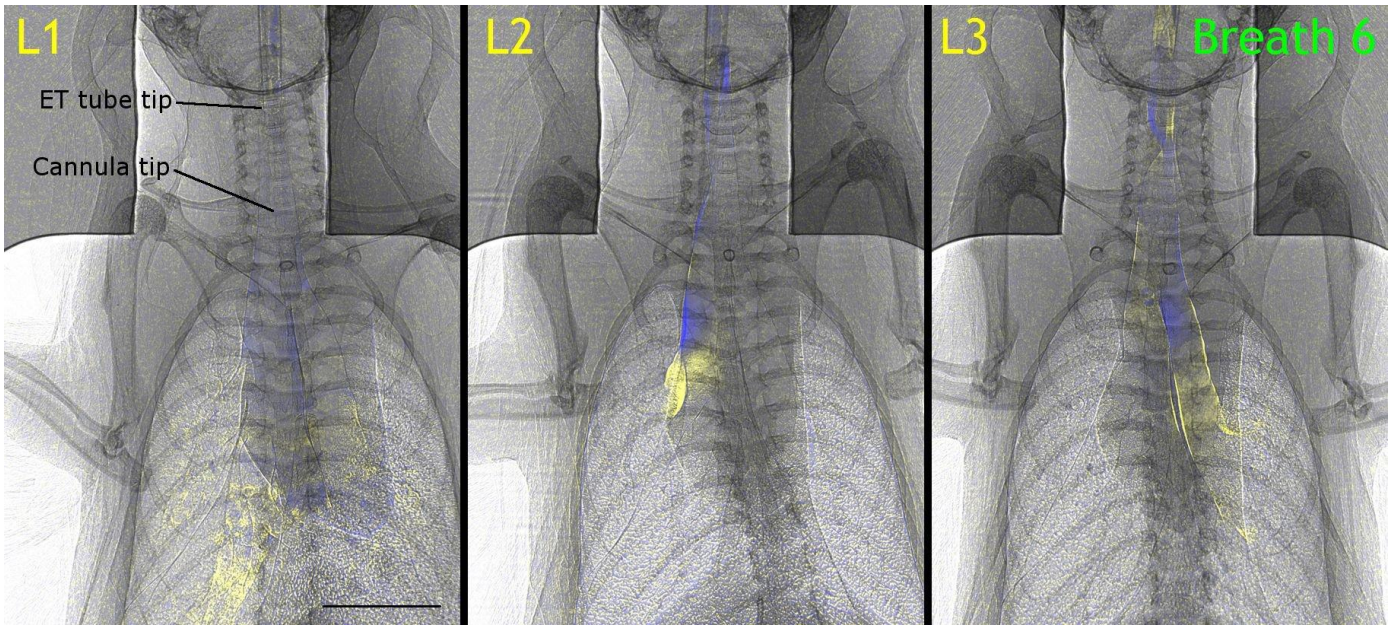


**Figure 4 | Fifteen microliter fluid dose rapidly delivered into mouse trachea**

The location of the initiation of a 15 µl dose delivered quickly over 3.6 seconds (shown at six breaths after delivery initiation, i.e. ~ 1 sec after delivery ceased). The location of the cannula tip and ET tube tip are marked for mouse L1. Only 3 mice are shown for the fast delivery, mouse L4 in was not imaged due to technical issues. Images are taken from Supplementary Video 4.

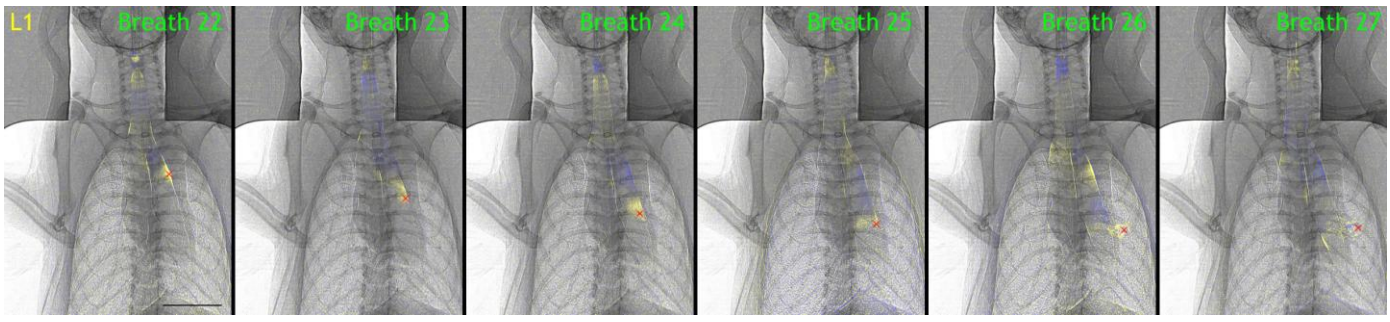


**Figure 5 | Fluid movement in lung conducting airways**

Six breaths from one mouse (L1 in Figure 4, which received 15 µl of fluid over 30 seconds) starting 22 breaths after dose initiation showing a bolus of fluid, marked with a red X, moving down the left main bronchus.

## SUPPLEMENTARY FILES

The supplementary files contain movie sequences showing the fluid motion in the mouse nose and lung, and are the source of the images shown in Figures 1-4. Each video shows 5 frames of baseline image collection, after which the fluid dose was delivered. All videos are Quicktime MP4 files, were encoded using the H.264 codec and can be played using the free VLC Media Player (available at http://www.videolan.org/vlc/).

### Supplementary Video 1 | Four microliter fluid dose in mouse nasal airways

The distribution of a standard fluid instillation (4 µl of 1:1 iomeprol and water mixture) is captured at 1 Hz in six different mice, for the period starting 5 seconds before a 10 second delivery, then imaged for a further 20 seconds. The pseudo-coloring of each frame image results was produced by a background subtraction algorithm referenced to the first (pre-delivery) image. Compared to the reference frame, the red/yellow shows areas with increased contrast present, and the purple/blue color being regions where contrast has been lost.

The variability of the dose distribution is apparent; for example, mice N1, N2 and N4 produced similar movement of dose into the right anterior, and lateral olfactory regions, while deliveries for mice N5 and N6 show the reduced depth of a smaller dose, due to droplet formation on the cannula tip that withheld that portion of the dose. Mouse N3 reveals the dose reaching the ipsilateral side of the nasopharyngeal meatus, and partial movement of dose into the eustachian tube (the postero-lateral point of fluid that forms at the 15 and 16 second frames). The nose in this mouse developed with a right-sided curvature, a deformity sometimes noted in these inbred mice. Despite this anatomical variability the 4 µl dose remains unilateral and did not pool at the nostril tip except for mouse N6 where the fluid bridges to the nose tip during delivery and then runs along the tooth bar.

### Supplementary Video 2 | Twenty microliter fluid dose in mouse nasal airways

Ten minutes after the 4 µl dose, a 20 µl dose of the same fluid was delivered to each mouse over 30 seconds (mouse N6 was removed due to its death under anesthesia just prior to the start of

imaging). The effects of this dose are immediate, reaching into the nasopharynx and progressing past the epiglottis and into the trachea. Formation of a large droplet that was subsequently inhaled intro both nostrils (mouse N2, N5) quickly filled the nasopharynx, but even one-sided slow instillations resulted in the dose spreading past the epiglottis. It is apparent that this volume produced broader reactions in all mice, as shown by the purple/blue colored areas of movement of the hair, skin, head and sometimes (e.g. mouse N1) the jaws. In some mice airway patency is lost, and no air movement occurs for periods over 30 seconds, and retrograde fluid movement is also seen, probably due to a snorting reaction to the instilled fluid.

**Supplementary Video 3 | Fifteen microliter fluid dose in mouse trachea**

A 15 µl fluid dose is delivered into the trachea over 30 seconds, after a 5 breath baseline period. When fluid is first expelled it moves retrograde along the cannula and the ET tube (breaths numbered 0-5) and thereafter dosed fluid (visualized as yellow/blue areas) can be seen entering the trachea and in some cases moving down the trachea and the mainstem bronchi. Some fluid movement occurred after the end of delivery (e.g. mouse L2 breaths 35-45, mouse L3 breaths 35-50.

**Supplementary Video 4 | Fifteen microliter fluid dose rapidly delivered into mouse trachea**

The same 15 µl volume was delivered over only 3.6 seconds, producing more immediate fluid delivery into the mainstem bronchi and to the deeper lung regions. Again, some retrograde dose loss occurred via the ET tube. Mouse L1 reacts to this dose with lung and body movement (apparent as the blue/yellow ghosting effect of body, bones and lung) while gross movements in mice L2 and L3 are not affected over this period. Fluid boluses move into the deeper lung until approximately breath 18, approximately 13 breaths after the end of dose delivery.